MATHEMATICAL MODELING AND COMPUTING, Vol. 11, No. 3, pp. 856–869 (2024)

Study and analysis of partial shading effect on power production of a photovoltaic string controlled by three different MPPT techniques: P&O, PSO and ANN

Atillah M. A.[1], Stitou H.[1], Boudaoud A.[1], Aqil M.[1], Hanafi A.[2]

[1]*Engineering and Applied Physics Team (EAPT), Superior School of Technology, Sultan Moulay Slimane University, Beni Mellal, Morocco*
[2]*Industrial Technologies and Services Laboratory, Higher School of Technology, Sidi Mohamed Ben Abdellah University, Fez, Morocco*

(Received 5 January 2024; Revised 4 September 2024; Accepted 6 September 2024)

Partial shading occurs when some of the solar panels are exposed to reduced irradiation. Partial shading can lead to creating peaks and troughs in power production. The goal of this study is to compare the effect of partial shading on the capacity of maximum power point tracking (MPPT) methods, to find the global maximum power point. To this end, the study focuses on performance simulation and discussion of Perturb and Observe (P&O), Particle Swarm Optimization (PSO), and Artificial Neural Network (ANN) controls. Analysing the three MPPT controller's results, in terms of accuracy, the ANN and PSO controls showed high performance. On the other hand, the P&O control showed lower accuracy, particularly under partial shading. For the speed of reaction, the P&O and ANN controls proved to be the fastest, while the PSO control showed a slightly longer response time. However, it is important to note that ANN approach presents added complexity in terms of conception.

Keywords: *renewable energy; MPPT techniques; photovoltaic energy; P&O; PSO; ANN.*
2010 MSC: 68Q30, 68T05, 68T07, 68T20, 90C59 **DOI:** 10.23939/mmc2024.03.856

1. Introduction

Irradiation and temperature have a direct impact on the efficiency of photovoltaic panels [1]. A rise in temperature or a decrease in irradiation lowers the maximum power output of photovoltaic panels, thus the use of MPPT [2]. Its concept is to position the operating point at maximum power [3], by acting on the photovoltaic panel's voltage or current. There are 3 main categories of MPPT techniques [2]:

— Conventional methods: simplicity is their hallmark [4]. However, they are limited to simple applications [5]. The most widely recognized controls are Incremental Conductance (InCond), P&O and Hill-Climbing (HC).
— Soft computing approaches: these are technically advanced methods, comprising 3 categories [6]. Methods based on artificial intelligence (AI) such as fuzzy logic (FL) and (ANN), Metaheuristic Algorithms (MA) [7] such as PSO, Grey Wolf Optimizer (GWO), Bat Algorithm (BA), Artificial Bee Colony Algorithm (ABC), and chaotic optimization algorithms (COA) such as Stepped-Up Chaos Optimization (SCO) [8].
— Hybrid approaches: combining different MPPT technology to benefit from different techniques [8]. Like PSO with P&O, ANN with P&O, GWO with P&O and ANN with InCond.

Our research is characterized by an intensive comparative study of technologies from two families: conventional and soft computing approaches. One future area of research will be hybrid methods.

The purpose of our paper is to examine three techniques capabilities and benchmarks them in relation to precision, sensitivity and reaction time under partial shading.

The article is organized as follows: Section 2 describes the methodologies and materials, while Section 3 discusses the results, the conclusion is in Section 4.

2. Methodology and materials

2.1. Photovoltaic system description

2.1.1. Photovoltaic generator

The PV model is as follows [13]:

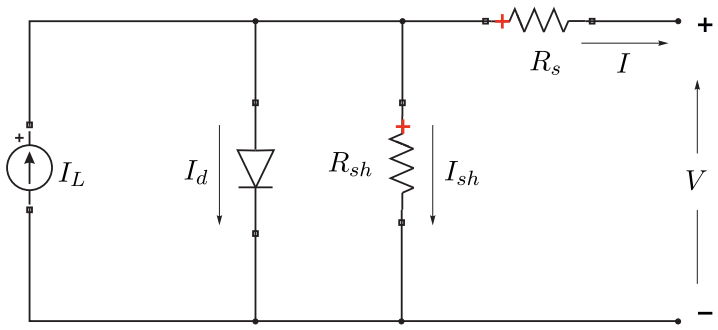

Fig. 1. Model of PV solar cell.

The photovoltaic cell model equation is as follows [14]:

$$I = I_L - I_{sh} - I_d.$$

If we replace I_d and I_{sh} with their corresponding terms, we get [14]:

$$I = I_L - \frac{v + I \cdot R_s}{R_{sh}} - I_0 \left(e^{\frac{q(v+I\cdot R_s)}{nkT}} - 1 \right),$$

where I_L is the photocurrent, I_d is the current through the diode, I_{sh} is the current P-N junction of diode, q is the charge on electron ($1.6022 \cdot 10^{-19}$ C), k is Boltzman constant ($1.3806 \cdot 10^{-23}\,\mathrm{J \cdot K^{-1}}$, n is factor of ideality, T is the absolute temperature in Kelvin, I_0 is the saturation current of diode, R_{sh} is represents P-N junction of diode, R_s is the overall resistance of the semi-conductor material and interconnections.

Figure 2 shows the PV panels employed.

In this study we use 4 photovoltaic panels connected in series, with a total maximum output power of 1708 watts. Figure 3 shows the characteristics of the photovoltaic array plotted a fixed temperature of 25°C.

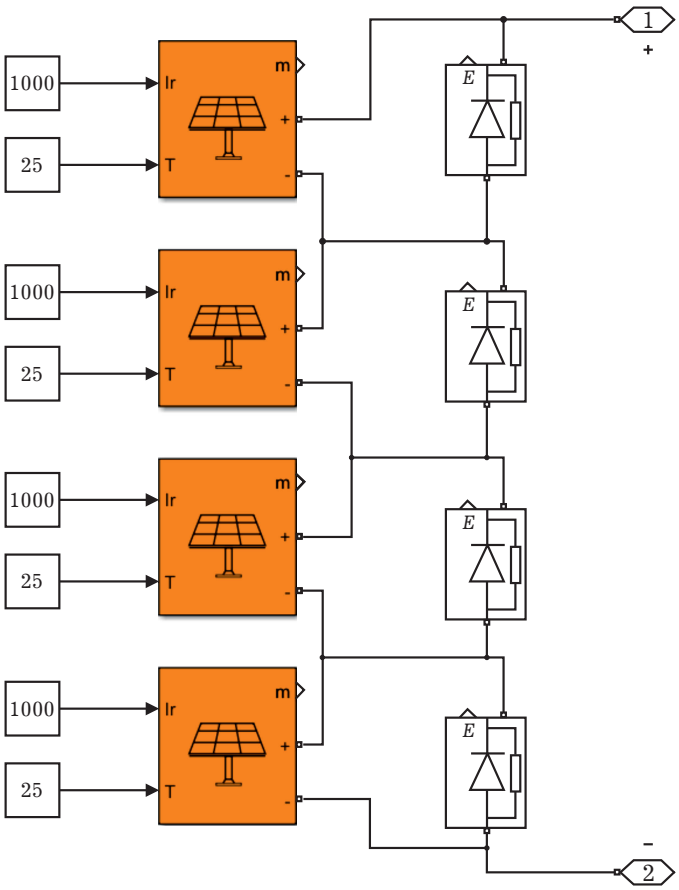

Fig. 2. The photovoltaic arrays employed in the study.

The graphs show a clear direct relation between irradiance and maximum power output. The maximum power increases proportionally with irradiance [15].

If the photovoltaic panel is not uniformly irradiated because of obstacles, this is known as partial shading [16]. This phenomenon leads to significant variations in the electrical characteristics of the system [17], as can be seen in Figure 4.

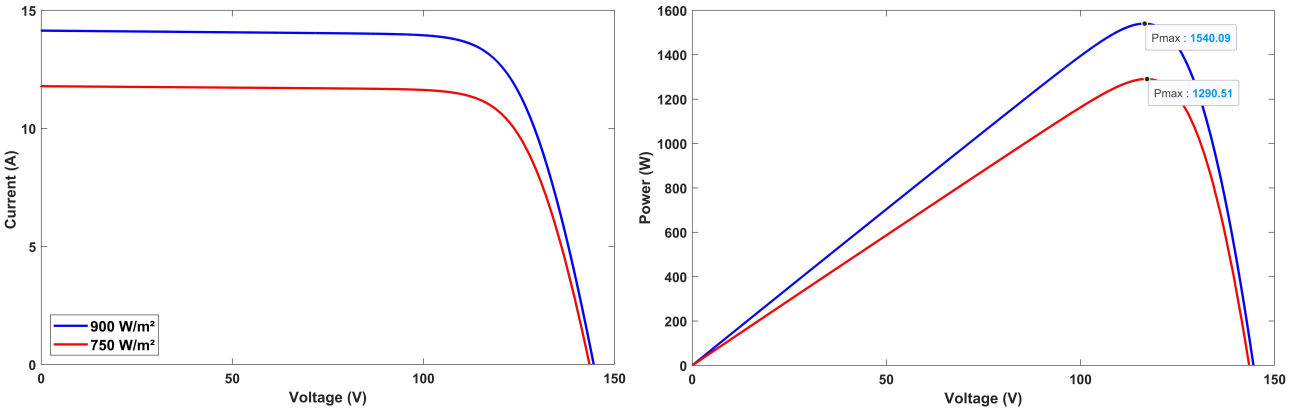

Fig. 3. PV array current-voltage and power-voltage characteristics for two irradiations levels.

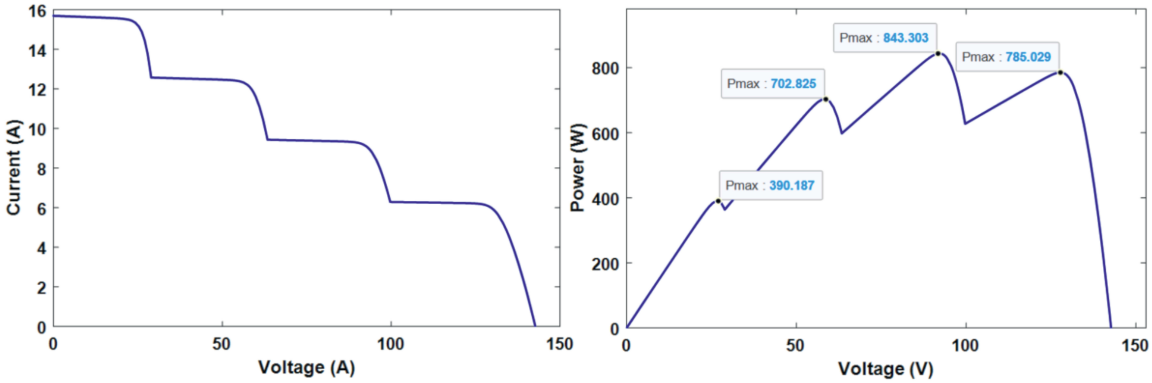

Fig. 4. PV array current-voltage and power-voltage under partial shading.

The graphs were plotted at 25°C, and each panel in series was irradiated differently. In particular, the first was irradiated by 400 W/m^2, the second by 600 W/m^2, the third by 800 W/m^2 and the fourth by 1000 W/m^2. The curve of power shows four different peaks (one global and three local) [18].

2.1.2. DC-DC converter (boost)

PV panels offer low output voltage, so the boost converter is essential to minimize the number of panels that have to be installed in series [19].

Therefore, the DC-DC converter is necessary with a control system to ensure that the photovoltaic array achieves its optimal working point. Figure 5 illustrates the boost converter [14].

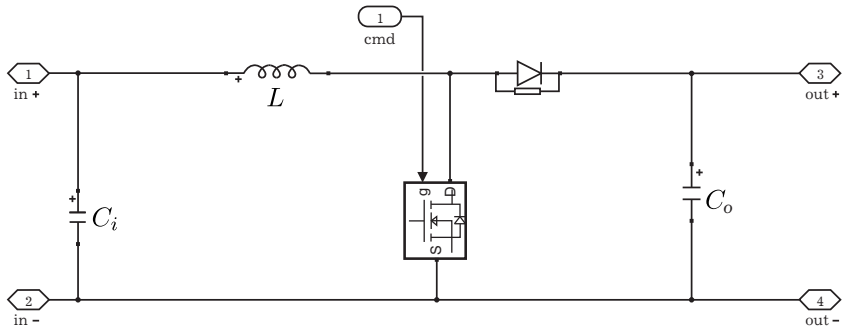

Fig. 5. The boost converter.

Inductance and capacitor values are obtained using the following equations [14]:

$$C_i = \frac{D \cdot I_o}{f_s \cdot \Delta V_i}, \quad C_o = \frac{D \cdot I_o}{f_s \cdot \Delta V_o}, \quad L = \frac{D \cdot V_i}{f_s \cdot \Delta I},$$

where D is duty cycle, f_s is switching rate, ΔV_i is ripple of input voltage, ΔV_o is ripple of output voltage, ΔI is ripple of current.

The values of the designed components are as follows: $C_i = 304\,\mu\text{F}$, $C_o = 12\,\mu\text{F}$, and $L = 2.4\,\text{mH}$. The relation between output voltage and input voltage is [14]:

$$V_o = \frac{V_i}{1 - D}.$$

We use a resistor ($R = 49.32\,\Omega$) on the boost output.

2.2. MPPT methods

2.2.1. Perturb and observe (P&O)

The P&O is the widely used control of tracking the maximum power point in photovoltaic applications [5]. Its advantages reside in its simplicity of implementation. The underlying principle involves systematic perturbation of PV voltage or current, then observing the resulting direction of power change [20], in order to determine the maximum power point, by following the slope of the power-voltage curve.

Figure 6 shows the algorithm of the P&O controller [21].

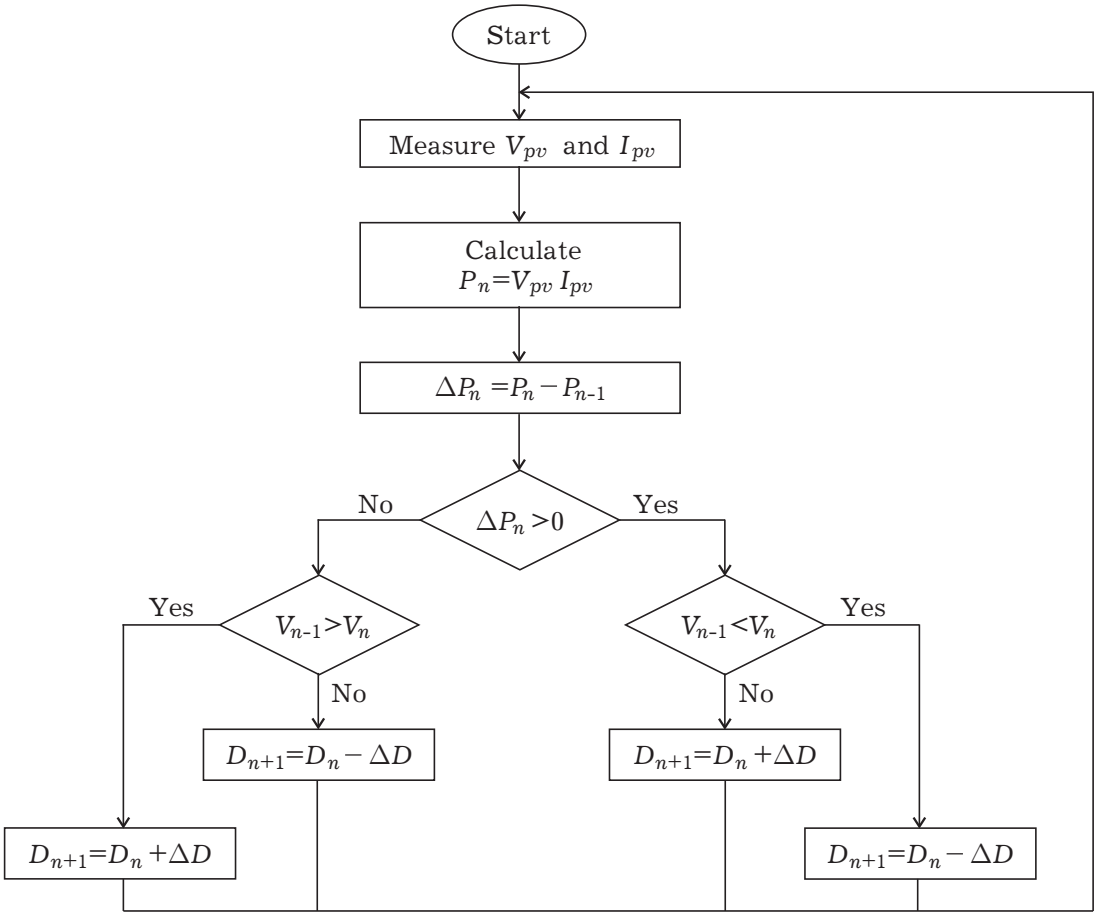

Fig. 6. The principle of P&O, where P_i is actual value of power, V_i is actual value of voltage, D_i is actual value duty cycle, ΔD is step size of duty cycle.

The system simulation using MATLAB Simulink is displayed in Figure 7.

2.2.2. Particle swarm optimization (PSO)

PSO approach is a random optimization technique, inspired by the organization of fish swarms or flights of birds. The PSO approach begins with a number of random solutions named particles [22]. The particles move within a search zone to reach the best solution [23].

In MPPT case, duty cycle represents the particle position, and the power of the photovoltaic panels represents the objective function.

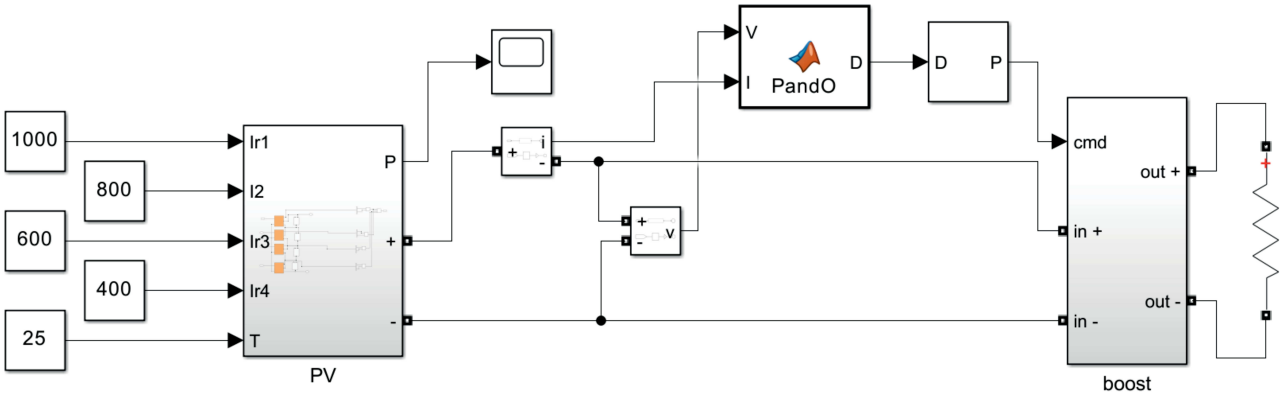

Fig. 7. P&O method simulation.

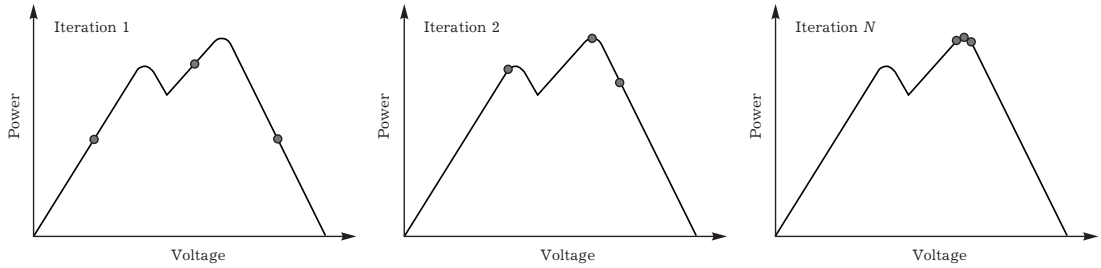

Fig. 8. Example of PSO MPPT Searching for MPP.

In our study, 3 particles are considered. The next steps explain how the PSO works [22]:

— Initialization of particles: the duty cycle is set randomly for each particle [17].
— Measurement of power: for each duty cycle the power values are measured [24].
— Updating the best position: save the duty cycle value corresponding to the maximum power [17].
— Updating particle positions: updating particle positions with the best position found in the preceding step [24].
— Repetition of process: power measurement, best positions and particle position updating are iterated many times [24]. At each repetition, the particles flow towards the duty cycle which maximizes power.

The parameters of the PSO method are essential to its success [17]:

— Particles number: determines the possible solutions in the searching area.
— Velocity components: is composed of various elements, such as the actual velocity, the best personal position of the particle (P_{pbest}) and the best position of the group (G_{best}).
— Coefficients of acceleration: C_1 and C_2 respectively determine the weight of the (P_{pbest}) and (G_{best}) elements in the particle velocity update.

The properties of the PSO approach are expressed by two equations below [22]:

$$P_{pi}(n+1) = P_{pi}(n) + V_{pi}(n+1),$$
$$V_{pi}(n+1) = WV_{pi}(n) + C_1R_1(P_{pbesti}(n) - P_{pi}(n)) + C_2R_2(G_{best}(n) - P_{pi}(n)),$$

$P_{pi}(n)$ is the i particle position, $V_{pi}(n)$ is the i particle velocity, n is the actual iteration, W is weight of inertia, R_1 and R_2 are random values in the range of $[0, 1]$, C_1 is cognitive coefficient, C_2 is social coefficient, P_{pbesti} is each particle best position, G_{best} is the best position of all the particles, the PSO principle is illustrated by the flowchart [22], in Figure 9.

The choice of limiting the number of particles to three in the PSO algorithm is aligned with the specific objective of targeting the global peak. The decision to limit the number of particles to three results from the nature of the problem, where the emphasis is on identifying the global maximum power point rather than exhaustive exploration of local peaks. This choice is also motivated by a pragmatic

consideration of computational resources, where the use of a small number of particles optimizes the balance between search quality and computational constraints.

The choice of specific values, $W = 0.4$, $C_1 = 1.2$, and $C_2 = 2$, is the result of an iterative process involving several tests. These values were set after a series of experiments aimed at finding the optimum combination offering the best results.

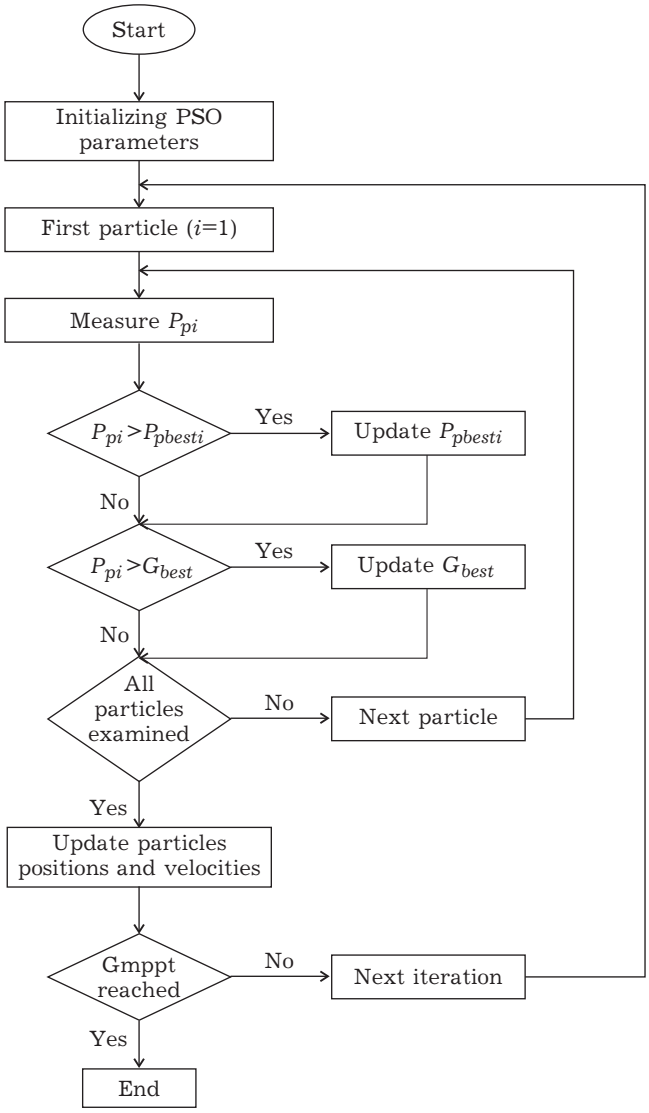

Fig. 9. The principle of PSO MPPT.

The acceleration coefficients, C_1 and C_2, play a key role in the balance between local and global exploration of solutions. A higher C_1 favors in-depth exploration around local peaks, while a higher C_2 encourages in-depth exploitation of the global peak. In addition, the coefficient of inertia W contributes to the stability of PSO convergence. The chosen value reflects a relatively low inertia, favoring controlled exploration of the search space. Low inertia limits particle oscillations, stabilizing convergence towards the point of maximum power.

The PSO-based MPPT control was simulated using MATLAB Simulink. As displayed in Figure 10.

2.2.3. Artificial neural networks (ANN)

ANN control principle. The ANN approach is inspired by the functioning of biological neurons [25]. In contrast to traditional methods, ANN is capable of learning from the information and turning it into cognition [26]. ANN is composed of elementary interconnected elements known as neurons [25].

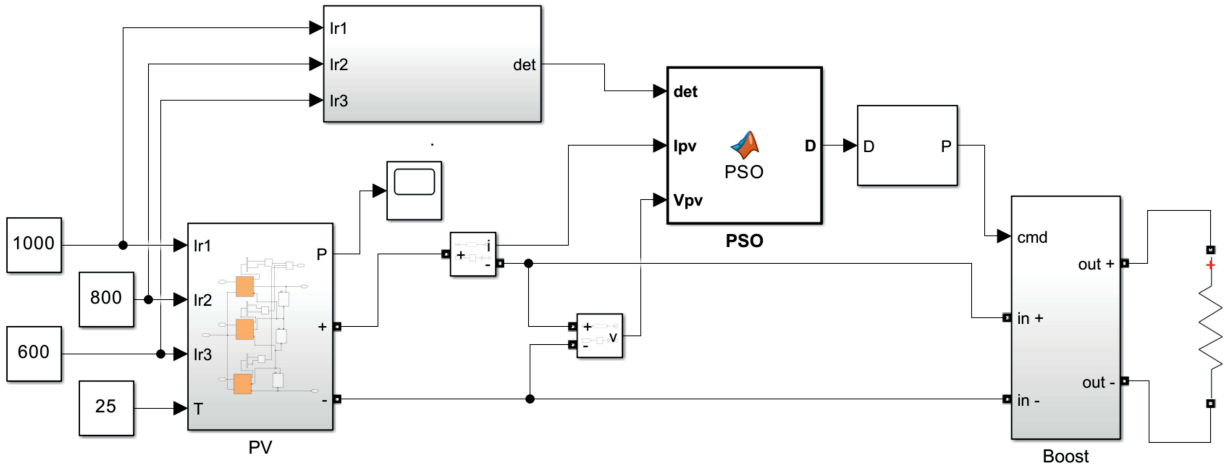

Fig. 10. PSO simulation.

There are three main stages in creating a neural network [13]:

— Collection of data: a practical database is assembled with the input and output examples concerned [26].
— Selection of architecture: determine how many hidden layers there are, how many neurons in each layer and the suitable activation techniques [26].
— Training and test/validation: weights and biases of the network are adjusted during training to reduce an error measure, like the MSE (Mean Square Error) [26]. Following training, the model is tested to determine its performance in terms of generalization and accuracy.

The ANN-based MPPT principle is described in Figure 11. Based on irradiance and temperature, the ANN generates the voltage equivalent to the maximum power point, which is later targeted by a fuzzy logic controller that regulates overall system output to achieve the maximum power point.

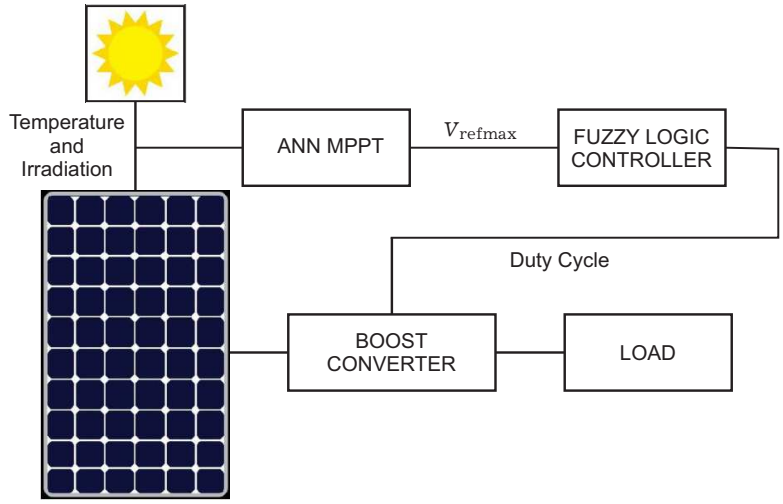

Fig. 11. The ANN MPPT design.

ANN control design. To collect the training data, we used a simulation of the photovoltaic panels in MATLAB SIMULINK under a constant value of 25 degrees Celsius, and extracted the value of maximum power point voltage (V_{mp}) by using a loop program, while also saving the irradiance levels associated. In total, 40000 values were registered in the table. Table 1 shows the selection of these values.

The algorithm is trained using the collected data [27].

We used the Levenberg–Marquardt algorithm for the training step. 50% of the data was assigned to training, 25% to validation data and 25% to test data.

Table 1. Obtained data selection.

Irradiation of Pv1 (W/m^2)	Irradiation of Pv2 (W/m^2)	Irradiation of Pv3 (W/m^2)	Irradiation of Pv4 (W/m^2)	Voltage of MPP (V)
401	729	278	127	92.92
770	550	532	915	121.96
649	656	874	825	121.96
619	264	316	898	58.08
125	541	251	981	60.98
742	550	524	153	90.02
714	138	164	570	58.08
187	837	836	750	87.12
235	694	567	976	92.92
684	821	508	489	121.96

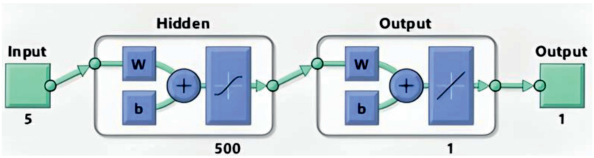

Fig. 12. ANN structure.

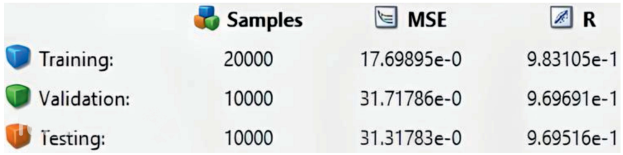

Fig. 13. ANN training results.

The regression coefficient was around 0.98. Analyzing the model's performance, a MSE of around 17.69 was observed during the learning phase. In the validation and test phases, the mean square error climbed to around 31. However, even with this increase, the level stays tolerable, suggesting a satisfactory generalization capability of the model.

In the previous steps, we discussed in detail the design of our MPPT system based on ANN. This neural network was trained to generate the reference voltage corresponding to the MPP as a function of solar irradiance and temperature values. To ensure that the system works with this voltage, we use a fuzzy logic controller.

Fuzzy logic controller. The small-signal model of a boost converter is a non-linear function [28]. That is why we chose to use a fuzzy logic controller, as this type of controller does not need an exact mathematical model to operate efficiently. Instead, they are designed on the basis of general knowledge of the installation.

Fuzzy logic is a branch of artificial intelligence that has revolutionized the way computer systems deal with imprecise or uncertain information. Unlike traditional binary logic, where propositions are either true or false, fuzzy logic allows us to deal with concepts that may be partially true or partially false [29].

The Simulink schematic of the fuzzy logic controller is shown in Figure 14.

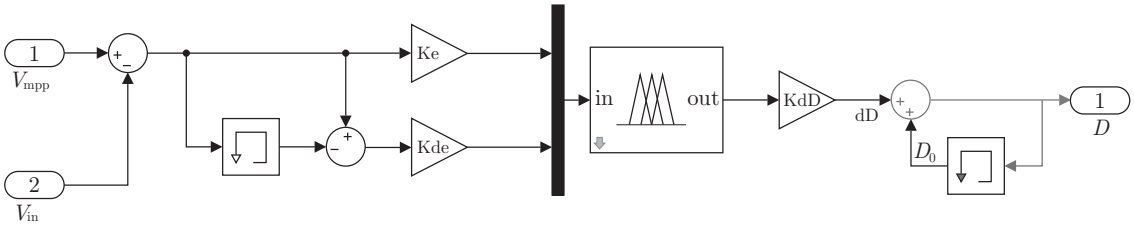

Fig. 14. Synopsis of fuzzy logic controller simulation.

The fuzzy logic controller takes two main inputs, the reference voltage, and the measured value. It calculates the error between them based on (1). And also considers the variation of this error given by (2). Using this information, the fuzzy logic controller algorithm makes a decision about the duty cycle adjustment,

$$E = V_{\text{mpp}} - V_{\text{in}}, \tag{1}$$

$$\Delta E = E - E_p, \tag{2}$$

where E is error, V_{mpp} is voltage corresponding to maximum power point, V_{in} is boost input voltage, ΔE is error variation, E_p is previous error.

The values of Ke, Kde and KdD are determined after several tests and iterations. After multiple iterations to find the optimum values, it was determined that the parameters offering the best response were set as follows: Ke = 1/300, Kde = 1/300 and KdD = 0.1.

The design of a fuzzy logic controller involves several stages. First, the choice of membership functions. These functions define how inputs are linguistically categorized within the fuzzy logic controller. Once the appropriate membership functions have been selected, the next step is to create a rule base. This rule base comprises a set of linguistic rules, which form the core element of a fuzzy controller.

Table 2. Obtained data selection, PB is positive big, PS is positive small, Z is zero, NS is negative small, NB is Negative big.

		Error variation				
		NB	NS	Z	PS	PB
Error	NB	NB	NB	NB	NS	Z
	NS	NB	NB	NS	Z	PS
	Z	NB	NS	Z	PS	PB
	PS	NS	Z	PS	PB	PB
	PB	Z	PS	PB	PB	PB

To design the rule base for the fuzzy logic controller output, various linguistic variables are identified and listed in Table 2 [30]. Next, the fuzzy controller is constructed and the membership functions and fuzzy rules are defined. We chose to use just five membership functions to simplify the controller's design and reduce its complexity. This decision was taken considering that the controller already offers satisfactory performance.

The membership functions for the input variables are illustrated in Figure 15, while Figure 16 shows the membership functions for output. For the rule bases a classic interpretation of Mandani was used. For the defuzzification method, we opted for the most widespread approach, namely Centroid Defuzzification, because of its simplicity and ability to deliver satisfactory results.

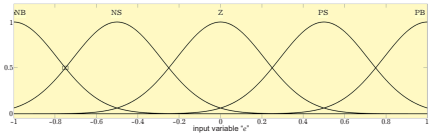

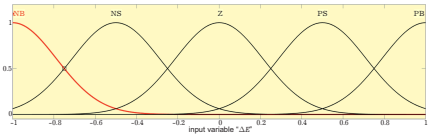

Fig. 15. The membership function plots of error and error variation.

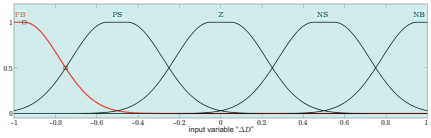

Fig. 16. The membership function plots of duty ratio.

After designing the ANN algorithm and the fuzzy logic controller, these two components were integrated into our system and simulated using MATLAB Simulink, as presented in Figure 17.

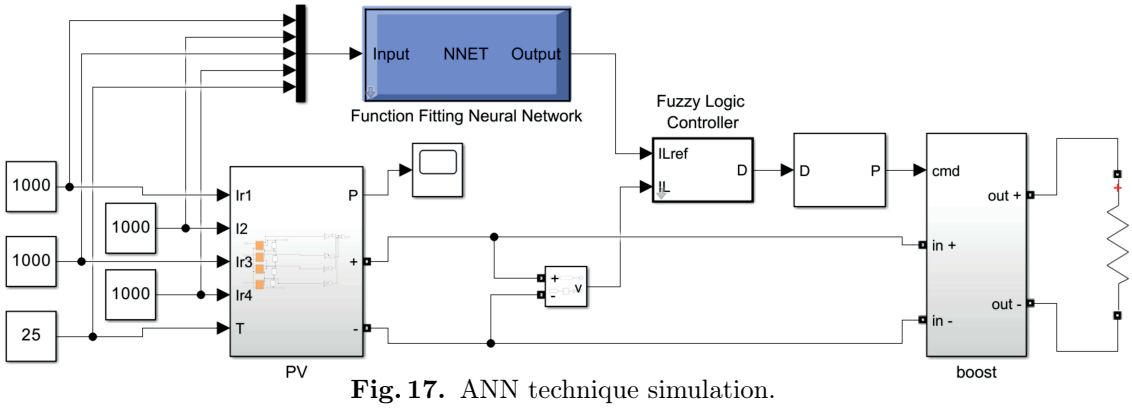

Fig. 17. ANN technique simulation.

3. Results and analysis

3.1. Simulation with uniform irradiation conditions

This part of the paper is dedicated to assessing the efficiency of MPPT methods mentioned above with uniform irradiation conditions. Three methods will be examined at the same irradiation levels, namely 900 and 750 W/m^2.

According to the power curves in Figure 3, the panel must be raised power of 1540 and 1291 W respectively.

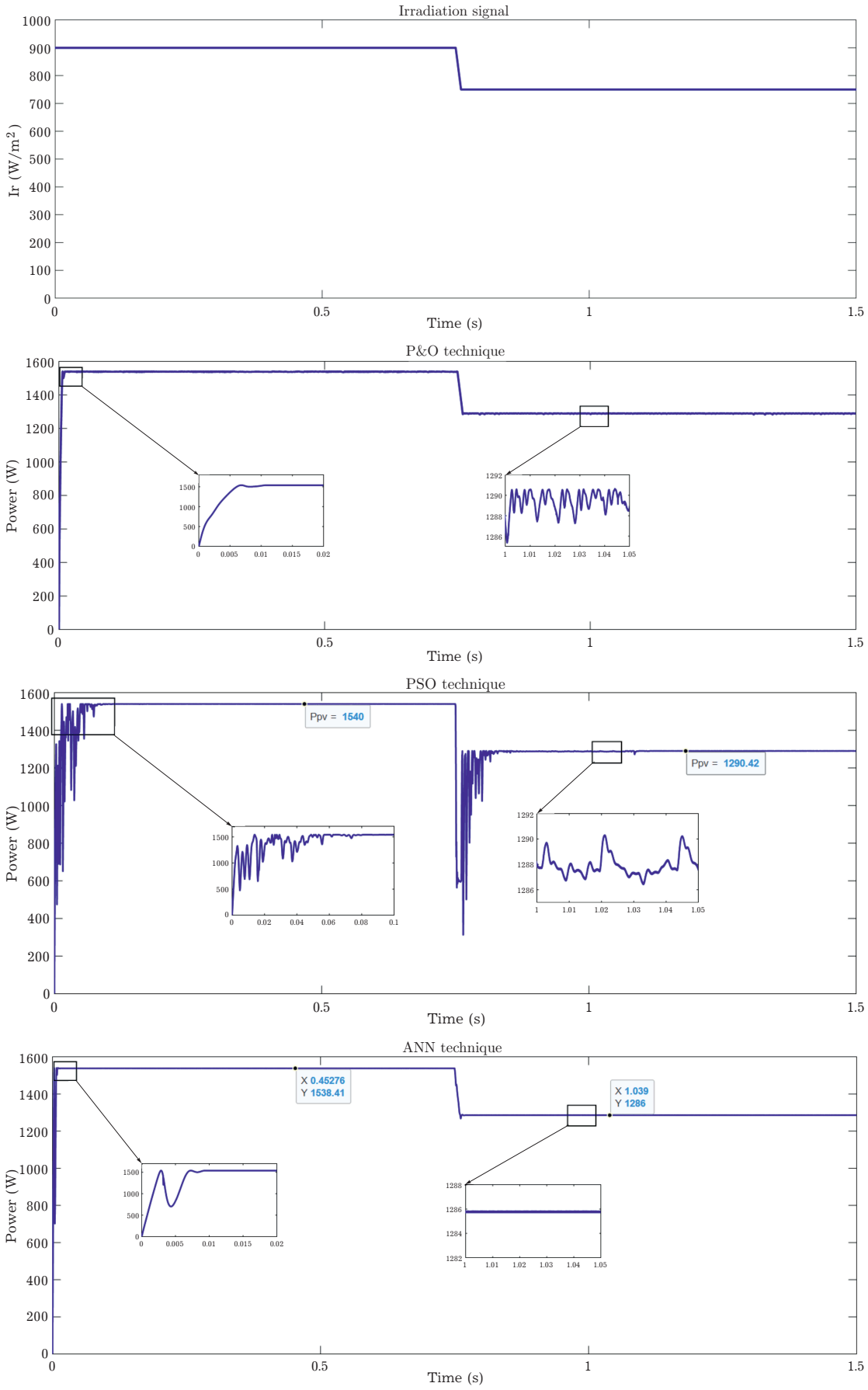

Fig. 18. PV power for the three techniques.

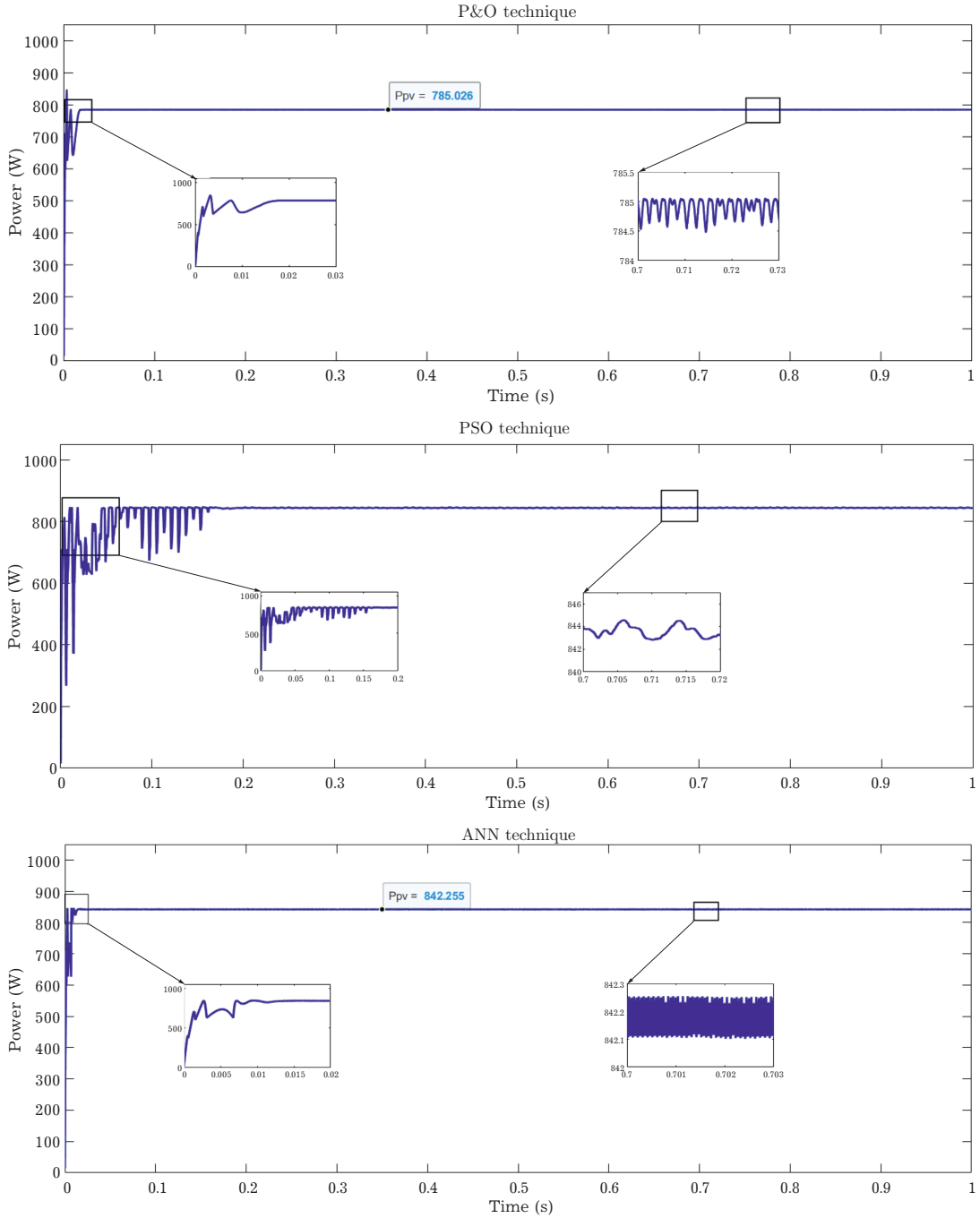

Fig. 19. PV power for the three techniques.

Table 3. Overview of system performance results.

	P&O	PSO	ANN
Pwoer response time (ms)	12	55	9
Power oscillations (W)	6	2.5	0.1
Power discrepancy (W)	1	1	5

Analysis of the results highlights the success of all three methods in tracking the maximum power point. This performance is a positive indicator of the effectiveness of the approaches considered under uniform irradiation.

In regard to rapidity of response, the results reveal that the ANN method stands out for its rapid reaction time. It is strongly preceded by the P&O, which also displays a notable responsiveness. In contrast, the PSO method is characterized by a relatively slower response time.

A point of attention emerges concerning the P&O, which, despite its speed, exhibits considerable oscillations around the MPP.

3.2. Simulation with partial shading conditions

After evaluating three methods with uniform irradiation, the methods will be evaluated with partial shading conditions, so the irradiation used for the panels is 1000, 800, 600 and 400 W/m^2 respectively.

Based on the PV panel characteristics displayed in Figure 4, the overall peak has a maximum power of 843.3 W.

Referring to Table 4, it is notable that the PSO and ANN successfully performing the system with high accuracy at the MPP. Conversely, the P&O method produces a local peak power of 785 W, resulting in reduced accuracy under conditions of partial shading.

Table 4. Overview of system performance results.

	P&O	PSO	ANN
Power response time (ms)	19	160	12
Power oscillations (W)	0.5	2	0.25
Power discrepancy (W)	58.3	0	1

The ANN method scores significantly higher than the PSO method in terms of response time. As a result, the ANN method seems to be the most appropriate of three methods tested, both in uniform irradiance and partial shading.

4. Conclusion

In this in-depth study, three MPPT methods, namely P&O, PSO and ANN, were carefully examined under a variety of climate scenarios. The results reveal that all methods showed a commendable ability to accurately track the point of maximum power under uniform irradiance conditions.

But when confronted with partial shading scenarios, the P&O method was limited by its sensitivity to local peaks. Conversely, both the PSO and ANN performed robustly, maintaining high accuracy. The ANN method in particularly stood out for its rapid response to disturbances.

On closer examination of the results, it is clear that the ANN MPPT method is the most effective. Its ability to effectively manage irradiation variations and provide rapid responses makes it a promising solution for real photovoltaic systems subject to dynamic conditions.

It should be noted, however, that the ANN method presents an increased complexity in its design. Moreover, as the number of panels to be managed increases, the conception becomes more difficult, both in terms of architecture and training. This also has an impact on implementation, which requires powerful devices for optimum performance.

The continual enhancement of MPPT methods stands as a paramount objective in the pursuit of optimizing the efficiency of PV systems.

Our future efforts will concentrate on two principal areas. Firstly, we will focus on exploring further the ANN MPPT method, extending its application to more complex setups encompassing various loads from off-grid systems to integration in grid-connected arrays. The main objective is to assess the resilience and performance of MPPT control in a variety of contexts, and thus provide valuable insights into its adaptability. Secondly, our research trajectory involves the investigation of new MPPT paths and methodologies to extract maximum benefits from photovoltaic systems. This involves incorporating advanced learning techniques and exploring hybrid approaches, such as the implementation of a neuro-fuzzy controller. These initiatives offer promising possibilities for refining existing performance parameters. The overall aim is to offer substantial advances in maximum power point tracking, which will enable significant progress to be made in improving the overall efficiency of photovoltaic systems. Our commitment to ongoing research and innovation underlines the imperative of constantly pushing the boundaries to unleash the full potential of solar energy harvesting technologies.

[1] Bingöl O., Özkaya B. A comprehensive overview of soft computing based MPPT techniques for partial shading conditions in PV systems. Mühendislik Bilimleri ve Tasarim Dergisi. **7** (4), 926–939 (2019).

[2] Kim S., Márquez J. A., Unold T., Walsh A. Upper limit to the photovoltaic efficiency of imperfect crystals from first principles. Energy & Environmental Science. **13** (5), 1481–1491 (2020).

[3] Li X., Wen H., Hu Y., Du Y., Yang Y. A comparative study on photovoltaic MPPT algorithms under EN50530 dynamic test procedure. IEEE Transactions on Power Electronics. **36** (4), 4153–4168 (2020).

[4] Pant S., Saini R. P. Comparative study of MPPT techniques for solar photovoltaic system. 2019 International Conference on Electrical, Electronics and Computer Engineering (UPCON). 1–6 (2019).

[5] Wasim M. S., Amjad M., Habib S., Abbasi M. A., Bhatti A. R., Muyeen S. M. A critical review and performance comparisons of swarm-based optimization algorithms in maximum power point tracking of photovoltaic systems under partial shading conditions. Energy Reports. **8**, 4871–4898 (2022).

[6] Al-Majidi S. D., Abbod M. F., Al-Raweshidy H. S. Design of an intelligent MPPT based on ANN using real photovoltaic system data. 2019 54th International Universities Power Engineering Conference (UPEC). 1–6 (2019).

[7] Yaich M., Dhieb Y., Bouzguenda M., Ghariani M. Metaheuristic Optimization Algorithm of MPPT Controller for PV system application. E3S Web of Conferences. **336**, 00036 (2022).

[8] Bollipo R. B., Mikkili S., Bonthagorla P. K. Hybrid, optimal, intelligent and classical PV MPPT techniques: A review. CSEE Journal of Power and Energy Systems. **7** (1), 9–33 (2020).

[9] Azad M. L., Sadhu P. K., Das S. Comparative study between P&O and incremental conduction MPPT techniques – a review. 2020 International Conference on Intelligent Engineering and Management (ICIEM). 217–222 (2020).

[10] Eseosa O., Kingsley I. Comparative study of MPPT techniques for photovoltaic systems. Saudi Journal of Engineering and Technology. **5**, 38–48(2020).

[11] Pal R. S., Mukherjee V. Metaheuristic based comparative MPPT methods for photovoltaic technology under partial shading condition. Energy. **212**, 118592 (2020).

[12] Tepe I. F., Irmak E. Review and comparative analysis of metaheuristic MPPT algorithms in PV systems under partial shading conditions. 2022 11th International Conference on Renewable Energy Research and Application (ICRERA). 471–479 (2022).

[13] Boudaraia K., Mahmoudi H., Abbou A. MPPT design using artificial neural network and backstepping sliding mode approach for photovoltaic system under various weather conditions. International Journal of Intelligent Engineering and Systems. **12** (6), 177–186 (2019).

[14] Bouri S., Mekkaoui O.-A., Mamem A. M. Comparative Study of Different MPPT Methods of a Boost Chopper of PV Generator. Acta Electrotechnica et Informatica. **22** (3), 24–31 (2022).

[15] Viswambaran V. K., Bati A., Zhou E. Review of AI based maximum power point tracking techniques & performance evaluation of artificial neural network based MPPT controller for photovoltaic systems. International Journal of Advanced Science and Technology. **29** (10s), 8159–8171 (2020).

[16] Belhachat F., Larbes C. PV array reconfiguration techniques for maximum power optimization under partial shading conditions: A review. Solar Energy. **230**, 558–582 (2021).

[17] Chtita S., Motahhir S., El Hammoumi A., Chouder A., Benyoucef A. S., El Ghzizal A., Derouich A., Abouhawwash M., Askar S. S. A novel hybrid GWO-PSO-based maximum power point tracking for photovoltaic systems operating under partial shading conditions. Scientific Reports. **12**, 10637 (2022).

[18] Vankadara S. K., Chatterjee S., Balachandran P. K., Mihet-Popa L. Marine predator algorithm (MPA)-based MPPT technique for solar PV systems under partial shading conditions. Energies. **15** (17), 6172 (2022).

[19] Raj A., Praveen R. P. Highly efficient DC-DC boost converter implemented with improved MPPT algorithm for utility level photovoltaic applications. Ain Shams Engineering Journal. **13** (3), 101617 (2022).

[20] Manna S., Akella A. K. Comparative analysis of various P & O MPPT algorithm for PV system under varying radiation condition. 2021 1st International Conference on Power Electronics and Energy (ICPEE). 1–6 (2021).

[21] Ghizlane C., Massaq Z., Abounada A., Mabrouki M. Speed Control of Induction Motor Driving a Pump Supplied by a Photovoltaic Array. International Journal of Renewable Energy Research. **10** (1), 237–242 (2020).

[22] Aassem Y., Hafidi I., Khalfi H., Aboutabit N. PSOBER: PSO based entity resolution. Mathematical Modeling and Computing. **8** (4), 573–583 (2021).

[23] Pathy S., Subramani C., Sridhar R., Thamizh Thentral T. M., Padmanaban S. Nature-inspired MPPT algorithms for partially shaded PV systems: A comparative study. Energies. **12** (8), 1451 (2019).

[24] Dagal I., Akin B., Akboy E. MPPT mechanism based on novel hybrid particle swarm optimization and salp swarm optimization algorithm for battery charging through simulink. Scientific Reports. **12** (1), 2664 (2022).

[25] Aqel F., Alaa K., Alaa N. E., Atounti M. Hybridization of Divide-and-Conquer technique and Neural Network algorithm for better contrast enhancement in medical images. Mathematical Modeling and Computing. **9** (4), 921–935 (2022).

[26] Mughal S. N., Sood Y. R., Jarial R. K. A neural network-based time-series model for predicting global solar radiations. IETE Journal of Research. **69** (6), 3418–3430 (2023).

[27] Ghedhab N., Youcefettoumi F., Loukriz A., Jouama A. Maximum Power Point tracking for a stand-alone photovoltaic system using Artificial Neural Network. E3S Web of Conferences. **152**, 01007 (2020).

[28] Zhang Y., Zhang Y. An advanced digital predictive valley current control algorithm for a boost converter. Journal of Physics: Conference Series. **1207**, 012001 (2019).

[29] Demkiv L. I., Lozynskyy A. O., Vantsevich V. V., Gorsich D. J., Lytvyn V. V., Klos S. R., Letherwood M. D. Fuzzy controller, designed by reinforcement learning, for vehicle traction system application. Mathematical Modeling and Computing. **8** (2), 168–183 (2021).

[30] Lorenzo J., Espiritu J. C., Mediavillo J., Dy S. J., Caldo R. B. Development and implementation of fuzzy logic using microcontroller for buck and boost DC-to-DC converter. IOP Conference Series: Earth and Environmental Science. **69**, 012193 (2017).

Дослідження та аналіз впливу часткового затінення на виробництво електроенергії фотоелектричного ланцюжка, керованого трьома різними методами MPPT: P&O, PSO та ANN

Атілла М. А.[1], Стіту Х.[1], Будауд А.[1], Акіль М.[1], Ханафі А.[2]

[1] *Команда інженерної та прикладної фізики (EAPT), Вища школа технологій, Університет Султана Мулая Сліман, Бені Меллал, Марокко*
[2] *Лабораторія промислових технологій та послуг, Вища технологічна школа, Університет Сіді Мохамеда Бен Абделлаха, Фес, Марокко*

Часткове затінення відбувається, коли деякі сонячні панелі піддаються зменшенню опромінення. Часткове затінення може призвести до створення вершин та впадин у виробництві електроенергії. Мета цього дослідження — порівняти вплив часткового затінення на здатність методів відстеження максимальних точки потужності (MPPT), щоб знайти глобальну максимальну точку потужності. З цією метою дослідження зосереджено на моделюванні продуктивності та обговоренні збурень та спостереження (P&O), оптимізації рою частинок (PSO) та керування штучною нейронною мережею (ANN). Аналізуючи результати трьох контролерів MPPT з точки зору точності, керування ANN та PSO показали високу продуктивність. З іншого боку, керування P&O виявило нижчу точність, особливо при частковому затіненні. Для швидкості реакції керування P&O та ANN виявилися найшвидшими, тоді як керування PSO виявило дещо довший час реакції. Однак важливо зазначити, що підхід ANN представляє додаткову концептуальну складність.

Ключові слова: *відновлювальна енергія; техніки MPPT; фотоелектрична енергія; P&O; PSO; ANN.*